Direct transport of midlatitude stratospheric ozone into the lower troposphere and marine boundary layer of the tropical Pacific Ocean

O. R. Cooper,[1] A. Stohl,[1,2] G. Hübler,[1] E. Y. Hsie,[1] D. D. Parrish,[3] A. F. Tuck,[3] G. N. Kiladis,[3] S. J. Oltmans,[4] B. J. Johnson,[4] M. Shapiro,[5] J. L. Moody,[6] and A. S. Lefohn[7]

Received 18 January 2005; revised 22 June 2005; accepted 1 September 2005; published 13 December 2005.

[1] The detailed survey of midlatitude stratospheric intrusions penetrating into the Northern Hemisphere tropics was one goal of the Pacific Sub-Tropical Jet Study 2004, conducted from Honolulu, Hawaii, during 19–29 January and 28 February to 15 March. Using the National Oceanic and Atmospheric Administration G-IV jet aircraft, instrumented with dropsondes and a 1-s resolution ozone instrument, we targeted an intrusion above Hawaii on 29 February. The data describe the strongest tropospheric ozone enhancements ever measured above Hawaii (in comparison to a 22 year ozonesonde record) and illustrate the mixing of stratospheric ozone into the midtroposphere as a result of convection triggered by the advection of relatively cold midlatitude air into the tropics. Measurements from the G-IV and Mauna Loa Observatory (3.4 km) show enhanced ozone in the lower troposphere, indicating that the remnants of the intrusion reached these levels. This conclusion is supported by a study using a stratospheric ozone tracer generated by the FLEXPART Lagrangian particle dispersion model. This paper also describes a similar intrusion that enhanced ozone at Mauna Loa on 10 March, as well as Honolulu, which is located in the marine boundary layer. G-IV flights in and out of Honolulu measured enhanced ozone associated with this event on several occasions. The 10 March event transported an estimated 1.75 Tg of ozone into the tropical troposphere, and we suggest that stratospheric intrusions that break away from the polar jet stream as they advect into the tropics are more effective at transporting ozone into the troposphere than intrusions that remain close to the polar jet stream in midlatitudes. Analysis of the dynamic conditions indicates that the frequency of stratospheric intrusions was not anomalous during January–March 2004. While the 10 March event was by itself an extreme event, strong stratospheric intrusions can be expected to influence the tropical lower troposphere in any year.

Citation: Cooper, O. R., et al. (2005), Direct transport of midlatitude stratospheric ozone into the lower troposphere and marine boundary layer of the tropical Pacific Ocean, *J. Geophys. Res.*, *110*, D23310, doi:10.1029/2005JD005783.

1. Introduction

[2] The chemical composition of the tropical troposphere has received a great deal of attention over the past 10 to 15 years to address issues of air quality on local, regional and global scales as well as to better understand the Earth's radiation budget. Ozone is an important trace gas affecting both photochemical and radiative processes and the impact of anthropogenic and biomass burning emissions on the tropical ozone budget has been well documented [*Fishman et al.*, 1990; *Lelieveld et al.*, 2001; *Thompson et al.*, 2001, 2003; *Lelieveld et al.*, 2004]. During the 1990s, researchers became aware that high ozone in the tropics could also have a stratospheric origin. *Hübler et al.* [1992] examined trace gas measurements from Mauna Loa Observatory (MLO) on the Island of Hawaii (3.4 km), during spring 1988. Free tropospheric ozone values reached as high as 78 ppbv and most of the free tropospheric air masses had O_3/NO_y correlations consistent with an upper tropospheric/lower stratospheric origin. During PEM-West A (Northern Hemisphere, late summer/early autumn), *Browell et al.* [1996] used airborne lidar measurements of ozone, water vapor and aerosol backscatter to identify air masses of stratospheric origin in the troposphere above the tropical North Pacific

[1] Cooperative Institute for Research in Environmental Sciences, University of Colorado–NOAA Aeronomy Laboratory, Boulder, Colorado, USA.
[2] Now at Department of Regional and Global Pollution Issues, Norwegian Institute for Air Research, Kjeller, Norway.
[3] NOAA Aeronomy Laboratory, Boulder, Colorado, USA.
[4] NOAA Climate Monitoring and Diagnostics Laboratory, Boulder, Colorado, USA.
[5] NOAA–University Corporation for Atmospheric Research, Boulder, Colorado, USA.
[6] Department of Environmental Sciences, University of Virginia, Charlottesville, Virginia, USA.
[7] A.S.L. & Associates, Helena, Montana, USA.

0148-0227/05/2005JD005783$09.00

Ocean. They concluded that stratospheric air masses with ozone in the 40–60 ppbv range could reach the lower troposphere down to 1 km and account for 27–40% of the lower tropospheric ozone in the central tropical Pacific. They suggested these air masses originated in midlatitude stratospheric intrusions that subsequently descended into the tropics via the climatological high-pressure system in the subtropical Pacific. In a related study of the Southern Hemisphere tropics during PEM-Tropics B, *Browell et al.* [2001] reached similar conclusions. *Weller et al.* [1996] launched a series of ozonesondes from a ship in the early 1990s, reported enhanced ozone in the middle and upper tropical troposphere of the Atlantic, and suggested a possible stratospheric origin, while *Tuck et al.* [1997] reported aircraft measurements of several trace gases in the tropical upper troposphere that indicated a clear midlatitude stratospheric origin.

[3] More recently, surveys of the large aircraft-based data sets produced by the PEM-West A and B, PEM-Tropics A and B and Measurement of Ozone and Water Vapor by Airbus In-Service Aircraft (MOZAIC) programs have shown that layers with trace gas and dynamic traits indicative of a stratospheric origin are commonly encountered throughout the tropical Pacific free troposphere [*Stoller et al.*, 1999; *Thouret et al.*, 2000, 2001]. Ozonesonde measurements from Hong Kong [*Liu et al.*, 2002], Indonesia [*Fujiwara et al.*, 2003] and Hawaii [*Oltmans et al.*, 2004] have also revealed cases of enhanced ozone layers in the middle and upper troposphere that were linked to a stratospheric origin. Furthermore, GOME retrievals and a trajectory study have associated enhanced tropospheric column ozone above Tahiti in the eastern South Pacific Ocean with a midlatitude stratospheric origin [*Ladstätter-Weißenmayer et al.*, 2004].

[4] Current research is also focusing on the actual mechanisms that transport ozone from the midlatitude stratosphere into the tropics. *Baray et al.* [2000] have shown that wintertime tropopause folding beneath the subtropical jet stream can lead to downward transport of stratospheric ozone into the tropical middle and upper troposphere. Similarly, Rossby wave breaking along the subtropical tropopause that leads to horizontal stirring of tropical and subtropical air masses has a maximum frequency in summer over the oceans and downstream of the subtropical high-pressure systems [*Postel and Hitchman*, 1999], and *Scott et al.* [2001] have shown that the resulting filamentation of stratospheric air can transport ozone into the upper tropical troposphere. In contrast to these summertime processes, *Waugh and Polvani* [2000] show that extratropical Rossby wave breaking can cause tongues of air with high potential vorticity (PV) to penetrate deep into the tropics, with a Northern Hemisphere maximum occurrence in January. These deep events have been shown to trigger convection along the leading edge of the PV tongue [*Kiladis*, 1998; *Waugh and Funatsu*, 2003] and to transport ozone into the upper troposphere above Hawaii [*Waugh and Funatsu*, 2003].

[5] To date, the most detailed case study of the transport of stratospheric ozone into the tropics describes a springtime cutoff low that broke away from the Southern Hemisphere subtropical jet stream and advected into the tropics above Africa as far north as 10°S [*Baray et al.*, 2003]. The feature persisted for about 2 weeks and slowly decayed. In contrast to a midlatitude cutoff low this system became detached from the stratosphere in both the horizontal and vertical planes. The authors argued that the irreversible detachment of the cutoff low from the stratosphere would deposit a significant amount of stratospheric ozone into the tropical troposphere. However, this conclusion could not be entirely confirmed as the study was limited by ozone measurements in the upper troposphere from a single ozonesonde at Reunion Island and two MOZAIC flights.

[6] Case studies of the mechanisms that transport midlatitude stratospheric ozone into the tropics have so far been limited to the mid and upper troposphere. While the measurements from MLO in the late 1980s and the Pacific aircraft-based studies of the 1990s have indicated that stratospheric air can impact the lower tropical troposphere (LTT), the enhancements were not particularly large and the transport mechanisms were not explored in detail. To the best of our knowledge, no study has yet shown that midlatitude stratospheric intrusions can have a distinct and strong impact in the tropical marine boundary layer. Given that stratospheric intrusions descend as they head equatorward approximately along isentropes that extend from the midlatitude stratosphere into the LTT it seems likely that ozone of stratospheric origin should have, on occasion, a very strong impact in the LTT. This hypothesis is supported by a 15-year climatology of cross tropopause exchange, showing that 4-day trajectories traveling from the midlatitude stratosphere into the tropical LTT have a maximum wintertime impact along a band stretching from Hawaii to Baja California [*James et al.*, 2003]. It also seems plausible that strong intrusions can descend into the marine boundary layer, perhaps aided by radiational cooling within the intrusion, convection and/or terrain turbulence effects of tropical islands.

[7] We hypothesized that wintertime stratospheric intrusions should have the potential to strongly impact LTT ozone, and that the lack of discussion in the literature on this topic was due to an absence of measurements that specifically target the intrusions as they decay in the tropics. To address this lack of data, the specific targeting of midlatitude stratospheric intrusions advected into the middle and lower tropical troposphere was one goal of the Pacific Sub-Tropical Jet Study 2004, an initiative of the National Oceanic and Atmospheric Administration (NOAA) Aeronomy Laboratory. The study occurred during 19–29 January and 28 February to 15 March and utilized the instrumented NOAA G-IV aircraft based in Honolulu, Hawaii. The G-IV was equipped with dropsondes and a 1-s resolution ozone instrument. Most of the flights out of Honolulu were dedicated to the separate Winter Storms Reconnaissance Program 2004 (WSRP), but 3 flights were reserved for exploring stratospheric intrusions. The first flight intercepted a stratospheric intrusion just north of Hawaii on 29 January. The third flight occurred in March and targeted low-altitude remnants of a stratospheric intrusion, but air traffic control prevented the aircraft from flying as low as was required. This paper describes the second flight, which occurred on 29 February and was designed to transect a midlatitude stratospheric intrusion that advected ozone into the tropics, directly above Hawaii. The data describe the

strongest tropospheric ozone enhancements ever measured above Hawaii (in comparison to a 22 year ozonesonde record) and illustrate the mixing of stratospheric ozone into the midtroposphere as a result of convection triggered by relatively cold midlatitude air advected into the tropics. Measurements from the G-IV and MLO show the ozone reached the LTT. This paper also describes a similar intrusion that enhanced ozone at MLO on 10 March and at Honolulu, which is located in the marine boundary layer. Operational G-IV flights out of Honolulu in support of WSRP captured enhanced ozone associated with this event on several occasions.

2. Method

2.1. NOAA G-IV Ozone and Dropsonde Measurements

[8] Ozone was measured on board the NOAA G-IV by a UV absorption instrument based upon the optical bench from a commercial instrument (TECO Model 49). The lamp, mirrors and signal processing electronics were replaced and the plumbing modified so that the instrument operated in a mode similar to that described by *Proffitt and McLaughlin* [1983]. One-second ozone measurements were made with a 1σ precision at standard temperature and pressure of approximately 1 ppbv.

[9] A series of 12 NCAR GPS dropsondes were released during the G-IV flight on 29 February. The dropsondes were designed by the National Center for Atmospheric Research, Boulder, and constructed by Vaisala Inc., Woburn, Massachusetts (Vaisala model RD93). These instruments measure temperature, dew point, pressure, and horizontal and vertical winds, and transmit the data back to the aircraft twice per second.

2.2. Hilo Ozonesondes

[10] The National Oceanic and Atmospheric Administration's (NOAA) Climate Monitoring and Diagnostics Laboratory (CMDL) has launched ozonesondes from Hilo on the Island of Hawaii on a weekly basis since 1982 (19.8°N, 155.0°W, 11 m). During special intensive periods to support field campaigns ozonesondes are launched more frequently. The balloon-borne ozonesondes were equipped with the widely used and tested electrochemical concentration cell (ECC) sensor [*Komhyr*, 1969; *Komhyr et al.*, 1995]. ECC sensors have an accuracy of about 10% in the troposphere, except when ozone is less than 10 ppbv when accuracies can be degraded to 15%. Personnel training and instruments were provided by the Ozone and Water Vapor Group of NOAA CMDL. See *Oltmans et al.* [1996] for an explanation of the equipment and techniques employed during this and many other studies. Prior to April 1998 the ozonesondes were prepared with a 1% buffered KI solution. Since April 1998 the ozonesondes were prepared with a 2% unbuffered KI solution. The different solutions can result in ozone differences of a few percent but these errors are negligible for our goal of simply identifying times when stratospheric ozone intrusions with high ozone mixing ratios were present above Hawaii. For direct comparison to the 1-s G-IV ozone measurements we only use Hilo data since 1991 when a digitized data recorder was first implemented to allow data collection at a high vertical and temporal resolution. The ozone, temperature and relative humidity data were partitioned into 100 m vertical layers, and reported as layer averages.

2.3. FLEXPART Stratospheric Ozone Tracer

[11] A stratospheric ozone tracer was calculated by the FLEXPART Lagrangian particle dispersion model [*Stohl et al.*, 1998; *Stohl and Thomson*, 1999], which simulates the transport and dispersion of linear tracers by calculating the trajectories of a multitude of particles. The model has been applied for case studies of trace gas transport [*Stohl and Trickl*, 1999; *Forster et al.*, 2001; *Stohl et al.*, 2003; *Forster et al.*, 2004] and a climatology of intercontinental transport [*Stohl et al.*, 2002; *Eckhardt et al.*, 2003]. The model was driven by data from the National Centers for Environmental Prediction (NCEP) Global Forecast System (GFS), with a temporal resolution of 3 hours (analyses at 0000, 0600, 1200, and 1800 UTC; 3-hour forecasts at 0300, 0900, 1500, and 2100 UTC), horizontal resolution of 1° × 1°, and 26 vertical levels. Particles are transported both by the resolved winds and parameterized subgrid motions. FLEXPART parameterizes turbulence in the boundary layer and in the free troposphere by solving Langevin equations [*Stohl and Thomson*, 1999]. To account for convection, FLEXPART uses the parameterization scheme of *Emanuel and Živković-Rothman* [1999], as described by *Seibert et al.* [2001].

[12] For the analyses in this paper the model was run from 12 January until 16 March 2004, including several days for spin-up time. For this simulation a special feature of FLEXPART was used, which creates a stratospheric tracer at the model boundaries that is then advected within the model domain [see *Stohl et al.*, 2000]. The domain covered eastern Asia, the North Pacific basin and North America from 1°S to 71°N and 99°E to 61°W. Every model column on the borders of this domain was split into about 100 layers where the mass flux of air was determined at every time step. For those grid cells along the domain border that experienced a net flux of air into the domain the mass of air flowing through these cells was calculated. Once the mass of air entering the model at a grid cell reached a certain threshold (M_{air}) a trajectory particle (or more, if required) was positioned at a random location at the boundary of the grid cell. The PV at this position was then determined by interpolation from the GFS data. Particles located in the troposphere were disregarded (PV < 2 potential vorticity units (pvu)). In contrast, stratospheric particles (PV > 2 pvu) were given a mass according to

$$M_{O_3} = M_{air} \cdot PV \cdot C \cdot 48/29$$

where $C = 60 \times 10^{-9}$ pvu^{-1} is the ratio between the ozone volume mixing ratio and PV in the stratosphere at this time of the year. The factor 48/29 converts from volume mixing ratio to mass mixing ratio. C was taken from *Stohl et al.* [2000] who found that the average relationship between ozone and PV in the lowermost stratosphere over Europe as determined from ozonesondes was between 58 and 69 ppbv/pvu between January and March.

[13] The particles were then allowed to advect through the stratosphere and into the troposphere according to the GFS winds. Once a particle reached an outflowing boundary of the domain it was removed from the simulation. At

any given time, approximately 40 million particles were advected within the model domain. This number fluctuated slightly, because the mass of air originating in the stratosphere varies with meteorological situation. Ozone was treated as a passive tracer and the simulation did not include chemistry or an ozone decay rate, but ozone was deposited at the surface according to a resistance scheme [*Wesely*, 1989]. Ozone fields were output every hour as 1-hour averages at a grid spacing of 0.75° × 0.75°. Grid cells were 500 m thick between the surface and 14 km, 1000 m thick from 14 to 16 km, and the top layer extended from 16 to 20 km. The output ozone fields only provide an estimation of the ozone enhancement due to transport from the stratosphere, and any mention of the stratospheric ozone tracer must be thought of as an enhancement to the typical tropospheric background ozone.

[14] The stratospheric ozone tracer was compared to the 1-min average ozone values from all of the G-IV flights through the lower stratosphere during the 2004 WSRP campaign (above the Pacific, between 15°N and 61°N). The model tended to overestimate ozone when measured ozone was between 100 and 400 ppbv, but underestimated ozone when measured values were greater than 400 ppbv. However, the geometric mean of all the point-by-point ratios of modeled/measured ozone was near unity (0.97), indicating little overall bias in the model. On a point-by-point basis, the standard error of the stratospheric ozone tracer compared to measured ozone was nearly a factor of 2, with much of the error attributed to relatively small errors in the position or timing of stratospheric features advected within the FLEXPART model. When this comparison is limited to latitudes north of 40°N, where the intrusions in this paper originated, the model underestimated ozone in the lower stratosphere with a mean modeled/measured ratio of 0.9; the standard error of the estimate improved to a factor of 1.5. The flux estimates discussed in Section 4 are for large intrusions covering several hundred square kilometers through much of the troposphere and originating north of 40°N. Therefore the estimated amount of ozone transported into the troposphere is expected to be 10% low, with an additional uncertainty of not more than a factor of 1.5.

[15] The FLEXPART stratospheric ozone tracer was also run in forecast mode during the experiment to assist with flight planning. The model was run four times per day using forecast wind fields from the 0000, 0600, 1200 and 1800 UTC runs of the NCEP GFS. Forecasts extended 120 hours and covered a slightly smaller domain than that described above and used fewer particles.

2.4. Auxiliary Animations

[16] Two auxiliary animations of the FLEXPART output are included with this paper.[1] While the animations are not essential for understanding the results presented here, viewing them allows the reader to clearly see the three-dimensional evolution of the midlatitude stratospheric ozone intrusions as they are transported into the tropics and subsequently decay. Animation 1 shows the evolution of the stratospheric intrusion sampled by the G-IV on 29 February 2004, represented by the 100 ppbv isosurface of the FLEXPART stratospheric ozone tracer. Similarly, Animation 2 shows the tropospheric evolution of the intrusion that impacted Mauna Loa on 10 March 2004 (100 ppbv isosurface). The animations can be viewed as animated GIFs or in QuickTime format with the QuickTime Player, freely available at http://www. apple.com/quicktime.

[1] Auxiliary material is available at ftp://ftp.agu.org/apend/jd/2005JD005783.

3. Results

3.1. The 29 February Flight

[17] The stratospheric intrusion sampled by the G-IV on 29 February 2004 originated several days earlier when a longwave trough formed along the polar jet stream above the western North Pacific Ocean on 26 February. By 1800 UTC, 27 February, the trough extended well into the tropics and had generated a midlatitude cyclone with its low-pressure center at 32°N (Figure 1a). A warm conveyor belt (WCB) formed on the eastern side of the trough and above the surface low, advecting clouds and moisture to the northeast; the associated high (cold) cloud tops are clearly visible in the GOES-West thermal IR channel (Figure 1a). West of the WCB the cyclone's dry airstream was advecting toward the southeast. This feature is evident in Figure 1b as a meridional dry air streamer depicted by the GOES layer average specific humidity, a derived product based on the GOES Imager water vapor channel [*Moody et al.*, 1999]. The feature is represented in the model fields by the PV contours on the 300 hPa surface. FLEXPART indicates that the stratospheric portion of the dry airstream contained high ozone mixing ratios (Figure 1c). The three-dimensional view of the ozone tracer 100 ppbv isosurface (Figure 1d) shows that the intrusion descended into the middle and lower troposphere (as low as 3.5 km at 21°N) as a continuous band from the midlatitudes into the tropics. By 1800 UTC, 29 February, the storm was isolated from the polar and subtropical jet streams with a PV anomaly and closed circulation aloft and a weak surface low located just west of the upper level low (Figures 1e and 1f). Similar to the PV anomaly, the FLEXPART ozone tracer shows that the ozone advected into the middle and lower tropical troposphere had also become detached from its higher-latitude reservoir (Figure 1g). However, the three-dimensional view of the ozone 100 ppbv isosurface shows that the intrusion slopes upward from west to east and the upper tropospheric portion is still attached to the stratosphere east of Hawaii. At this time the intrusion is not as visible in the GOES layer average specific humidity product (Figure 1f) as it has become overrun by relatively moist tropical air [*Wimmers and Moody*, 2004]. The animation of this intrusion (Animation 1) illustrates the southward motion of the ozone as the storm formed, followed by the intrusion's west-east elongation over Hawaii where it eventually detached from the stratosphere and dispersed.

[18] Midlatitude cyclones that extend into the North Pacific subtropics and tropics during the Northern Hemisphere cool season (October-March) are commonly known as kona storms [*Otkin and Martin*, 2004]. This particular cyclone fits the definition of a kona storm, and by 28 February it had become a classic kona low bringing heavy rainfall to what would normally be the leeward side of the Hawaiian Islands under typical trade wind conditions. During February 2004 the northwest corner of the Island

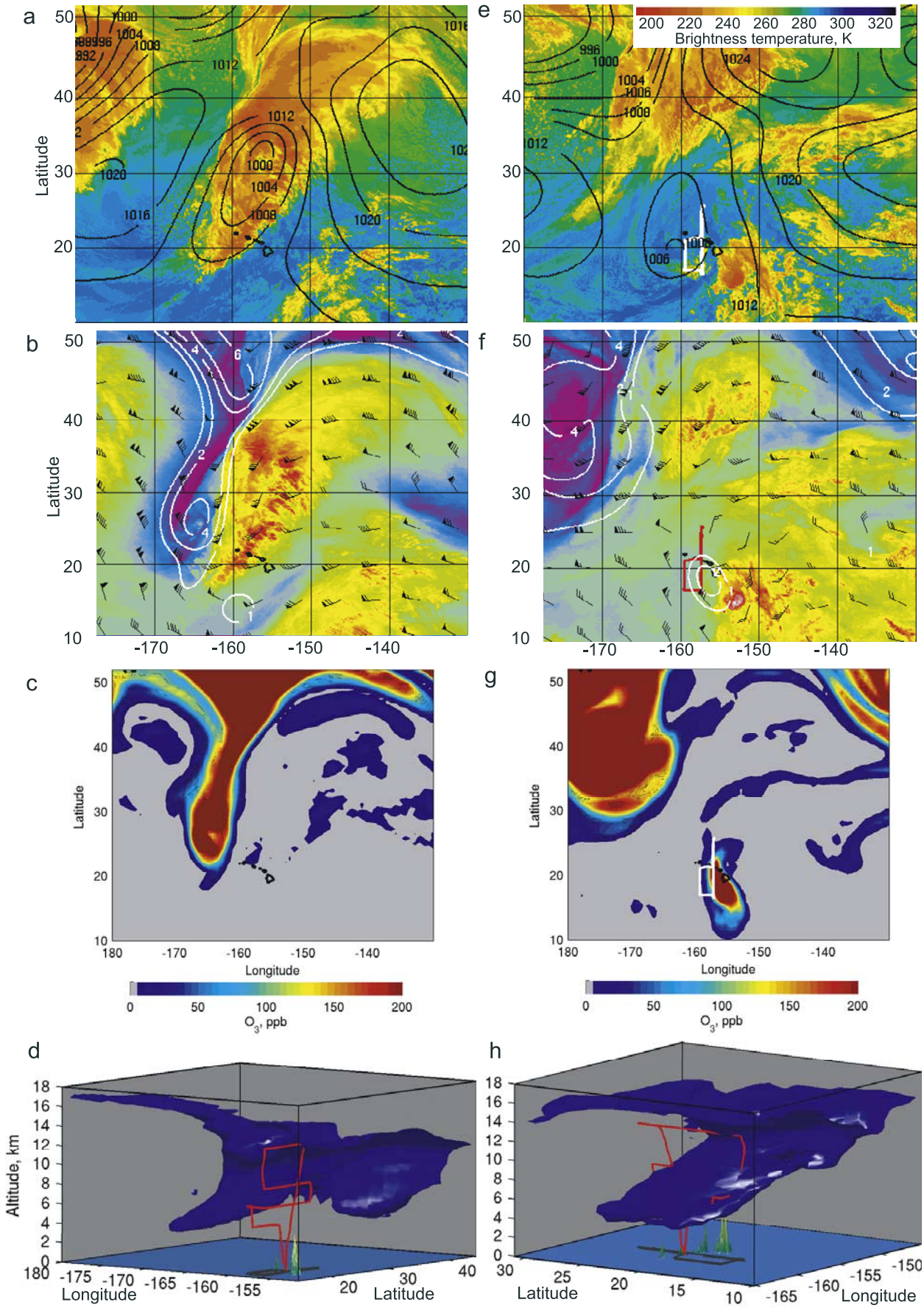
a
e
b
f
c
g
d
h
Latitude
Longitude
Brightness temperature, K
200 220 240 260 280 300 320
O_3, ppb
0 50 100 150 200
Altitude, km

Figure 1

of Hawaii received 200–300% of its normal February precipitation. Most of the excess precipitation was associated with this particular kona storm, with the rain gauge at Kona Village (Station Index 064765) receiving 14.5 cm of precipitation during 27–29 February, 97% of the monthly total [*National Oceanic and Atmospheric Administration*, 2004].

[19] By 1800 UTC, 29 February, the highest cloud tops were east of Hawaii, and Figure 1f shows that the high cloud tops are also east of the PV anomaly at the center of the kona storm, which is typical of extratropical longwave troughs that penetrate into the tropics [*Kiladis*, 1998]. Convective clouds and precipitation also occurred beneath the PV anomaly. Radiosondes from Lihue on the western side of the Hawaiian Islands showed that the ambient temperature between 2 and 7 km was 4°–10°C colder when the PV anomaly passed over the station in comparison to a quiescent period several days earlier. Similarly, dropsondes released from the G-IV into the convective region below the PV anomaly showed temperatures 4°–9°C lower than the reference period at Lihue. As a result of the cold air advection beneath the PV anomaly, values of convective available potential energy (CAPE) reached 700 m^2 s^{-2}, as calculated using the methodology of *Emanuel* [1994]. While modest in comparison to severe thunderstorms over the central United States, a CAPE value of 700 m^2 s^{-2} is consistent with tropical convection. We conclude that the cold air advected from midlatitudes beneath the PV anomaly destabilized the atmosphere causing convection and precipitation.

[20] Figure 2 shows the flight track that transected the intrusion, which was planned according to forecasts of the FLEXPART stratospheric ozone tracer. The G-IV took off from Honolulu just after 1700 UTC on 29 February and headed north as it ascended to a cruising altitude of 13 km. During the ascent the G-IV passed through the intrusion between 7 and 8 km with ozone reaching 100 ppbv. Upon reaching its cruising altitude the G-IV headed north to 26°N, turned and headed south to 16.9°N. During this transect the aircraft was just below the tropopause and successfully released 12 dropsondes between 25°N and 17°N at approximately 80 km intervals (Figure 2c). At this time the G-IV was above the intrusion and the ozone varied from 20 to 50 ppbv. After the dropsondes were released the G-IV flew two north-south transects through the intrusion at 8.9 km (ozone up to 280 ppbv) and 6.9 km (ozone up to 181 ppbv). To capture some of the east-west structure of the intrusion, the G-IV headed west at 6.9 km and then performed a short N-S transect at 4.8 km (ozone up to 91 ppbv) during its return to Honolulu.

[21] Figure 2 shows elevated ozone along the 8.9 and 6.9 km transects, with enhancements detected from 10.0 km (111 ppbv) down to 3.3 km (72 ppbv). The greater ozone values are associated with the very dry air within the intrusion (compare Figures 2a and 2b to Figure 2c). The southern half of the transect at 6.9 km has a great deal of ozone variability, ranging from 31 to 160 ppbv. Because of convection this portion of the flight track is much more moist than the regions of the intrusion sampled at 8.9 km or along the northern half of the 6.9 km transect. The convective cloud tops along this portion of the flight track are visible in Figure 3a, and the precipitation produced by the convection is shown in the radar image in Figure 3b. The temperatures of the convective cloud tops near the flight track, as determined by the GOES infrared imagery reached as low as 250 K which corresponds to an altitude of approximately 7.5 km, as determined from the dropsondes (Figure 2c) and confirmed by the G-IV flight scientist (coauthor, A. Tuck). Figure 4 shows the 1-s ozone measurements versus relative humidity. The data at 8.9 km were measured above the level of the convective cloud tops. They show a broad range of ozone but all measurements were in very dry air, with relative humidity values typically less than 20%, representing the transition between dry tropical midtropospheric air with low ozone and the dry ozone-rich polar stratospheric air advected into the tropics. The data at 6.9 km also have a wide range of ozone with greater values generally corresponding to dry air and the lower values generally corresponding to moister air. The range of data points in Figure 4 at this altitude fall along a pseudo mixing line, illustrating the transition from stratospheric air to moist tropical air. (Similar results were found when relative humidity was replaced by the conservative quantity of water vapor mixing ratio, allowing a true mixing line to be drawn between the dry and moist air.) Detailed time series for the portion of the flight track at 6.9 km (not shown) also indicate that ozone and relative humidity were anticorrelated with higher humidity and lower ozone values occurring near the convective clouds, as observed by the flight scientist. We conclude that the mixing between the stratospheric and tropospheric air at 6.9 km was mainly the result of deep convective clouds penetrating the base of the intrusion.

[22] Figure 5 shows the G-IV ozone time series with the corresponding FLEXPART stratospheric ozone time series interpolated to the flight track. In these types of comparison it must be remembered that the stratospheric ozone tracer only estimates the amount of ozone from the stratosphere while the ozone measurements represent various mixtures of stratospheric and tropospheric ozone. The ozone tracer tracks the measurements fairly well in the sense that high ozone corresponds to high tracer values and low ozone corresponds to low tracer values. There is very good agreement at 8.9 km between the ozone measurements and the ozone tracer with maximum ozone reaching 260 ppbv and maximum ozone tracer reaching 280 ppbv, indicating that the measured ozone is dominated by stratospheric ozone. The transect at 13 km shows the

Figure 1. (a) GOES-West infrared image with mean sea level pressure, (b) GOES-West layer average specific humidity product (purples and blues indicate dry air in the middle to upper troposphere) with 300 hPa IPV contours (contours at 1, 2, 4 and 6 pvu) and 250 hPa wind barbs, and (c) FLEXPART stratospheric ozone tracer at 9 km, 1800 UTC, 27 February 2004. (d) FLEXPART 100 ppbv ozone isosurface (blue) at 1800 UTC, 27 February, with the terrain of Hawaii (green) and the 29 February flight track (red) for scale. (e–g) As in Figures 1a–1c but for 1800 UTC, 29 February, with the 29 February flight track superimposed. (h) As in Figure 1d but for 2000 UTC, 29 February; note the different perspective and scale.

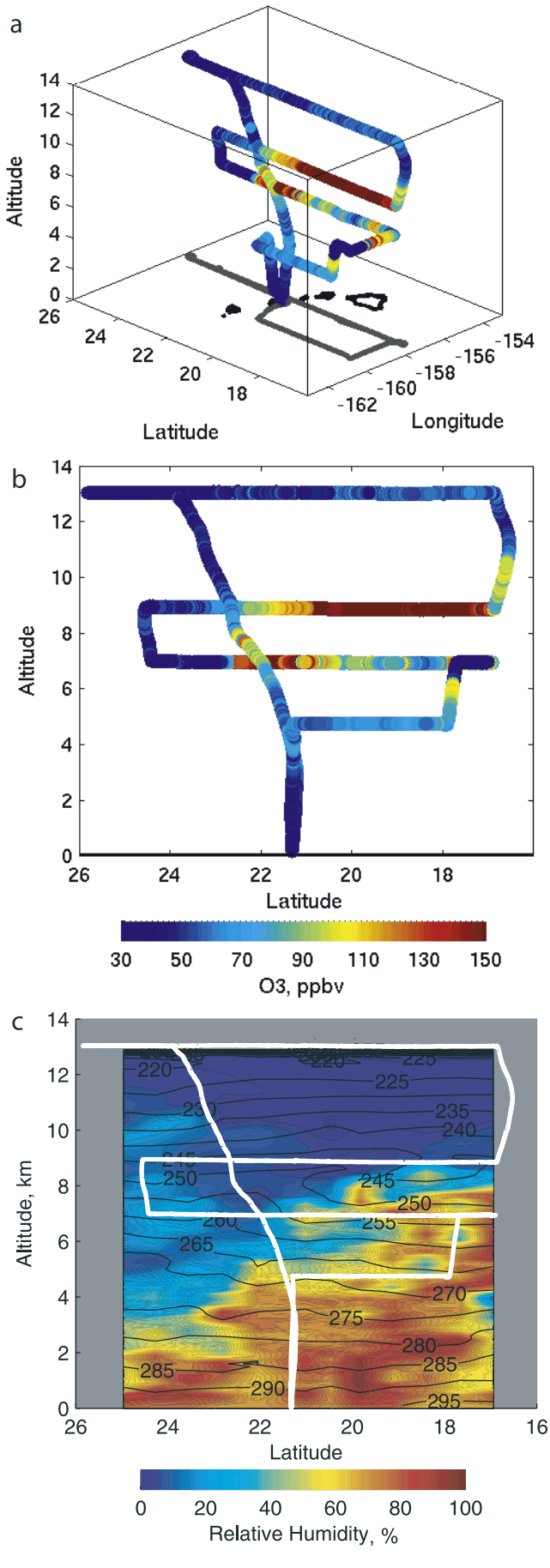

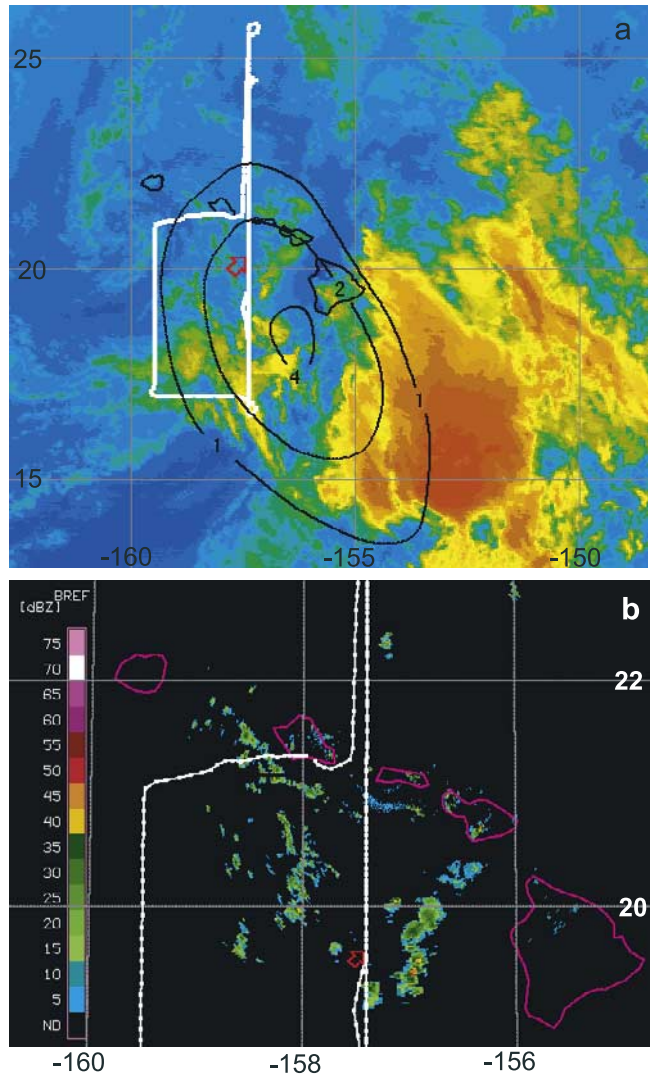

Figure 3. (a) GOES-West IR image at 2100 UTC, 29 February, showing the flight track (white line), the location of the G-IV at 2100 UTC (red arrow), and IPV on the 300 hPa surface (black contours) at 1800 UTC. See Figure 1e for the color scale. (b) Radar base reflectivity from the Molokai NEXRAD station at 2107 UTC, 29 February, with the flight track (white line) and the location of the G-IV (red arrow).

FLEXPART stratospheric ozone tracer exceeded measured ozone near 1900 UTC by 60 ppbv, which was the result of the flight track being very close to the boundary between the tropical and stratospheric air and the model shifting the boundary just a few km to the west into the

Figure 2. (a) Three-dimensional view of the 29 February flight track, colored by 1-s ozone measurements and showing the flight track shadow (gray) and the outline of Hawaii (black). (b) North-south cross section of the 29 February flight track colored by ozone. (c) North-south cross section of the flight track (white line) with the curtain of relative humidity (colored) and temperature (contours) measured by the 12 dropsondes.

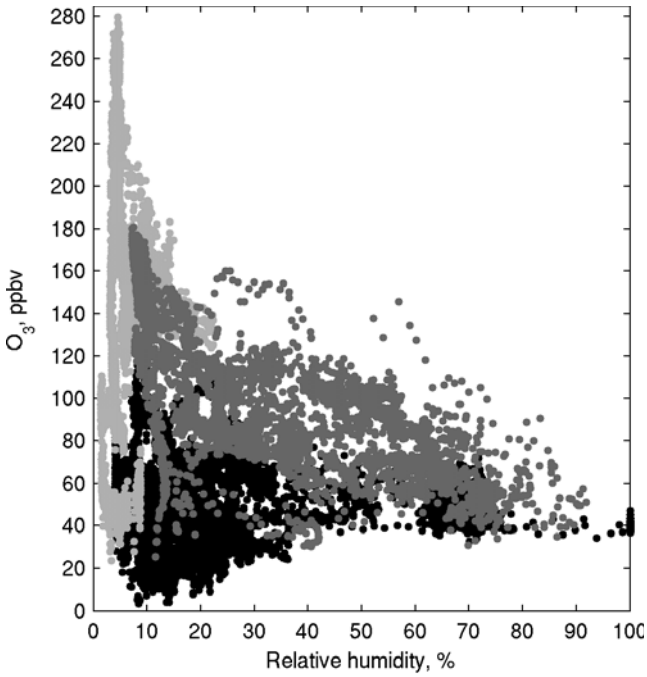

Figure 4. One-second ozone versus relative humidity measurements from the G-IV flight on 29 February 2004. Data measured near 8.9 km between 1900 and 2000 UTC are shaded light gray, data measured near 6.9 km between 2038 and 2145 UTC are shaded dark gray, and all other data are black.

path of the G-IV. During the ascent from Honolulu and along the transects at 6.9 and 4.8 km the modeled ozone exceeded measured ozone, sometimes by a factor of 2 or 3. These portions of the flight track were in the region of convection and we conclude that the over prediction may be the result of the model not simulating well enough the mixing and dilution generated by the convection.

[23] In Figure 6a, hourly average ozone and CO measurements at MLO (19.5°N, 155.6°W, 3.4 km) on the Island of Hawaii are displayed. Measured ozone reached a maximum of 81 ppbv at 1200 UTC on 29 February, with ozone elevated (>50 ppbv) from 0000 UTC, 29 February, to 0300 UTC, 1 March. The FLEXPART stratospheric ozone tracer was also elevated at this time with similar magnitudes indicating that much of the measured ozone was of stratospheric origin, except during the early hours of 29 February, when the ozone tracer overpredicted ozone at MLO by 20–30 ppbv. CO at MLO actually increased from 70 ppbv on 28 February to 83 ppbv at the time of the peak ozone enhancement. One might assume that CO should decrease when a stratospheric intrusion impacts MLO, but during winter there is typically more CO in the high-latitude lower stratosphere than in the tropical lower troposphere as shown by a plot of ozone versus CO from all of the MOZAIC flights during February 2004 (Figure 6c). These 1-min average data come from 167 flights between airports in Europe and airports in North America, Europe, Africa, Australia and Asia, representing over 1000 flight hours [*Nedelec et al.*, 2003]. Only data from the Northern Hemisphere and above 1 km altitude are shown. Data measured north of 50°N and above 8 km are highlighted in white to emphasize the ozone and CO mixing ratios typical of the upper troposphere and lower stratosphere north of the polar jet stream where the 29 February intrusion originated. Also shown are the ozone and CO mixing ratios from the LTT air mass that impacted MLO on 28 February (white cross), prior to the intrusion, and from the time when the stratospheric intrusion impacted MLO (black cross). A mixing line is drawn on the figure connecting the ozone/CO data point representative of MLO prior to the intrusion with a data point representative of the lowermost stratosphere (the data point representing the lowermost stratosphere is arbitrary and many different points could be selected). The ozone/CO data point representative of the intrusion at MLO lies very close to the mixing line, indicating that the ozone and CO values at Mauna Loa during the time of the intrusion are consistent with the concept of a lower stratospheric air mass descending to MLO and mixing with a LTT air mass.

[24] To address the issue of upslope winds affecting MLO, the CO data in Figure 6a are plotted for daytime (crosses) and nighttime conditions (solid circles), where the daytime period (1000–2200 Hawaii standard time) is susceptible to upslope winds that can advect local pollutants to MLO [*Hahn et al.*, 1992]. The nighttime CO values on 29 February and 1 March are as high as the daytime values, indicating that the overall increase in CO is not a local effect.

[25] Figure 6b shows ozone and the FLEXPART tracer at the Anuenue Fisheries site (21.3°N, 157.9°W, 3 m) on Sand Island, approximately 2 km west of downtown Honolulu (CO is not measured at this site). Measured ozone was elevated (>40 ppbv) on 28–29 February coinciding with the increase in stratospheric ozone tracer. The FLEXPART

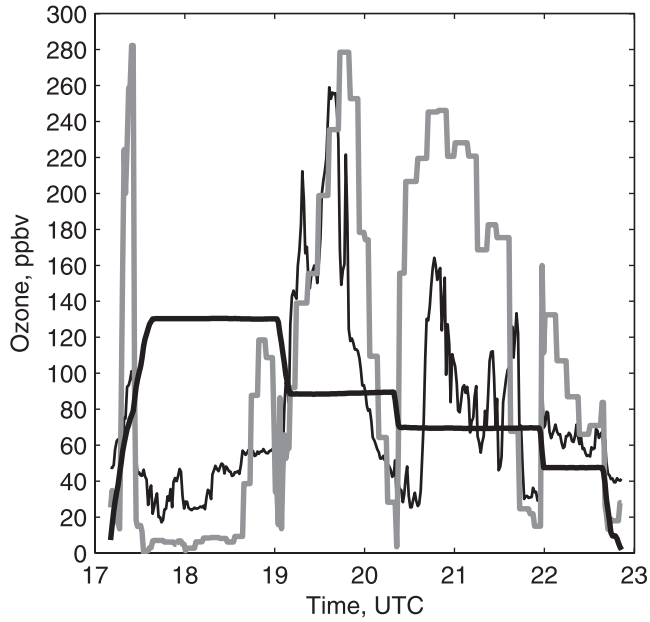

Figure 5. Comparison between minute-average ozone measured by the G-IV (thin black line) on 29 February and the FLEXPART stratospheric ozone tracer (gray line). The altitude of the G-IV is also shown (thick black line) in meters/100.

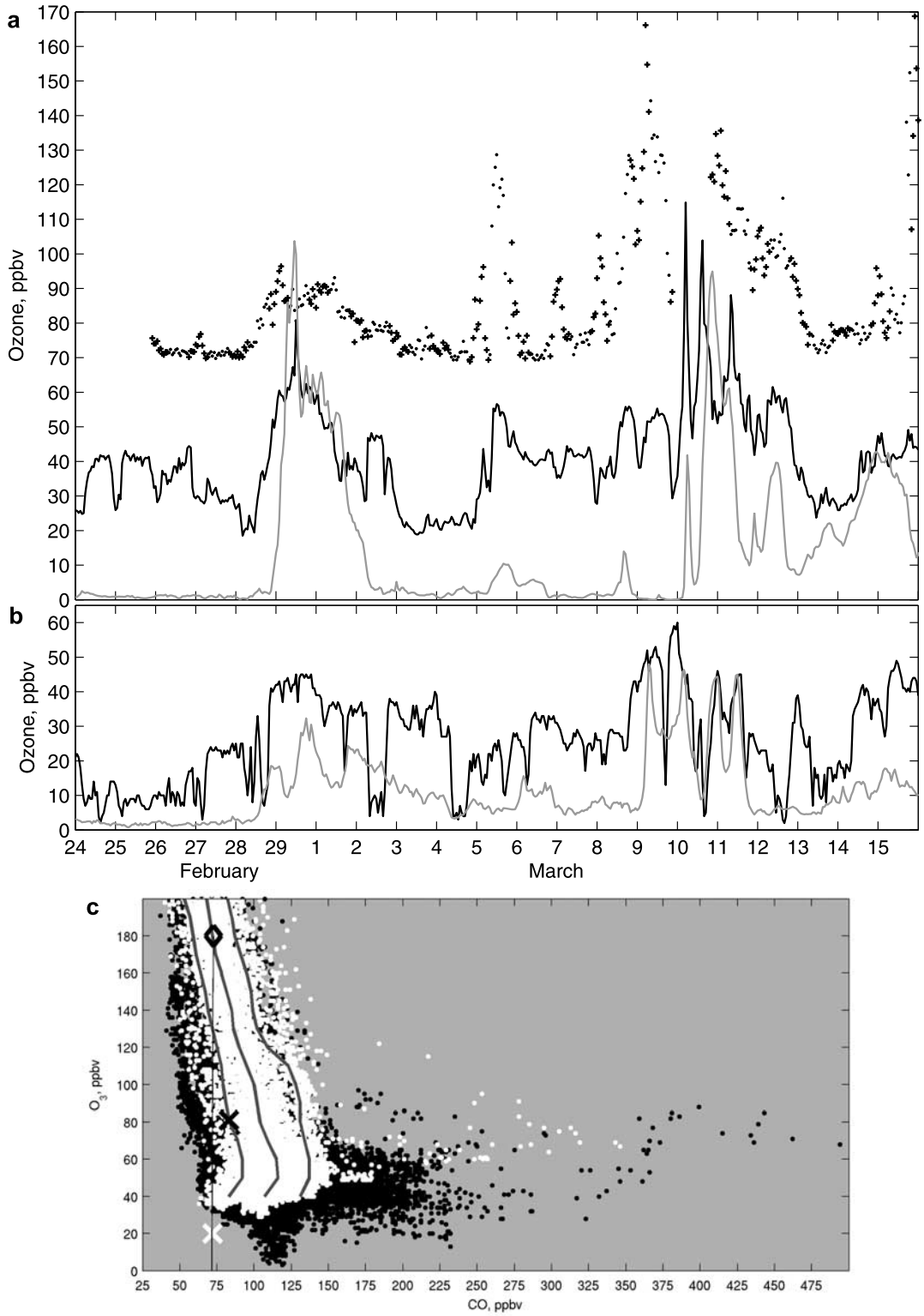

Figure 6. (a) Hourly average ozone (black line), CO (solid circles for nighttime and crosses for daytime), and FLEXPART stratospheric ozone tracer (gray line) at MLO. (b) Hourly average ozone (black line) and FLEXPART stratospheric ozone tracer at Honolulu. (c) Ozone versus CO from all Northern Hemisphere MOZAIC flights above 1 km during February 2004. Values measured north of 50°N and above 8 km are highlighted (white), and the gray lines indicate the 10th, 50th, and 90th CO percentiles for a given ozone value. Also indicated are the ozone and CO values at MLO for the early hours of 28 February (white cross) and the time of the ozone peak at MLO on 29 February (black cross). A mixing line connects the MLO data point (white cross) and an arbitrary point in the lower stratosphere (black diamond).

Table 1. Maximum Mass of Stratospheric Ozone Tracer at Several Layers in the Troposphere in the Vicinity of Hawaii (10°–23.45°N, 165°–145°W) During the 29 February and 10 March Stratospheric Intrusions, as Estimated by FLEXPART[a]

	29 February Event		10 March Event		Percent Increase From
	Maximum Tracer Mass, Tg	Date and Time	Maximum Tracer Mass, Tg	Date and Time	29 February to 10 March
0.0–1.0 km	0.07	0700 UTC, 1 March	0.10	1900 UTC, 10 March	43%
1.0–3.0 km	0.11	1000 UTC, 29 Feb.	0.18	1900 UTC, 11 March	64%
3.0–5.0 km	0.15	0600 UTC, 29 Feb.	0.21	0300 UTC, 12 March	40%
5.0–7.0 km	0.15	2100 UTC, 28 Feb.	0.18	1700 UTC, 11 March	20%
7.0–9.0 km	0.14	0500 UTC, 29 Feb.	0.17	2100 UTC, 11 March	21%
9.0–11.0 km	0.14	1200 UTC, 29 Feb.	0.27	1800 UTC, 10 March	93%
11.0–13.0 km	0.17	1000 UTC, 29 Feb.	0.38	1000 UTC, 9 March	124%
0.0–15.0 km	1.14 (0.68–1.54)	1000 UTC, 29 Feb.	1.75 (1.05–2.36)	1100 UTC, 11 March	54%

[a]The dates and times at which each maximum occurred are also indicated. The ranges of uncertainty for the 0.0–15.0 km estimates are given in parentheses.

stratospheric ozone tracer at the surface was a factor of 10 less then the quantity of tracer at 8.9 km along the flight track, indicating that the intrusion was diluted by a factor of 10 by the time it entered the marine boundary layer. Possible mechanisms for transporting the ozone into the marine boundary layer include convective down drafts [*Betts et al.*, 2002], and turbulent mixing associated with Hawaii's volcanic peaks extending above the marine boundary layer. While the enhancements at MLO and Honolulu are not extreme, it appears that this particular extratropical stratospheric intrusion contributed to the ozone mixing ratios in the LTT and tropical marine boundary layer.

3.2. The 10 March Intrusion

[26] The extratropical stratospheric intrusion that impacted MLO on 10 March 2004 was forecast by FLEXPART but was not directly targeted by the G-IV as the aircraft was dedicated to the separate WSRP experiment at that time. However, the intrusion was intercepted by the G-IV over several days as the aircraft took off and landed in support of WSRP.

[27] This intrusion formed in a similar manner to the 29 February intrusion as verified by animations of GOES water vapor imagery with PV overlays illustrating clear midlatitude longwave breaking (not shown). The evolution of the FLEXPART stratospheric ozone tracer during this event is illustrated in Animation 2. This intrusion transported more ozone to the tropics than the one sampled on 29 February. Table 1 shows the maximum amount of stratospheric ozone tracer at various levels in the troposphere in the vicinity of Hawaii (10° to 23.45°N; 165° to 145°W) for both the 29 February and 10 March events. Between 0 and 15 km the 10 March event contained 54% more stratospheric ozone tracer than the 29 February event. The 10 March event also contained more tracer at all sublayers between 0 and 13 km. The evolution of the 10 March event was slightly different from the 29 February event in that the maximum amount of tracer in the 0–1 km layer occurred 16 hours prior to the maximum in the 0–15 km layer, while the 29 February event caused a maximum in the 0–1 km layer 21 hours after the maximum in the 0–15 km layer.

[28] Figure 7 shows the ozone profiles from three G-IV flights out of Honolulu that intercepted the 10 March intrusion. Because of instrument initiation well after takeoff only one ascent and three descent profiles are available. All three flights detected ozone in excess of 90 ppbv below 5 km, and the locations of the flights with respect to the intrusion are shown in Animation 2. Figure 8 compares the ozone from these flights to the FLEXPART stratospheric ozone tracer. During the descent on 10 March the 1-s data showed an ozone maximum of 132 ppbv at 3 km (Figure 7) with relative humidity of 2% and a dew point temperature of −36°C, indicating that this midlatitude air mass had descended from a high altitude. However, this part of the intrusion was not captured by FLEXPART (Figure 8a). Animation 2 shows that concentrated quantities of the model tracer did not move into the flight track region until 12–15 hours later. FLEXPART did a better job of capturing the timing of the intrusion on 12 March and 13 March (Figures 8b–8d). However, the relative magnitude of the tracer enhancement varies from case to case, showing a thinner, taller peak than the ozone measurements in Figure 8b and smaller peaks than the ozone measurements in Figures 8c and 8d.

[29] The 10 March event made a greater impact at MLO than the 29 February event with hourly average ozone

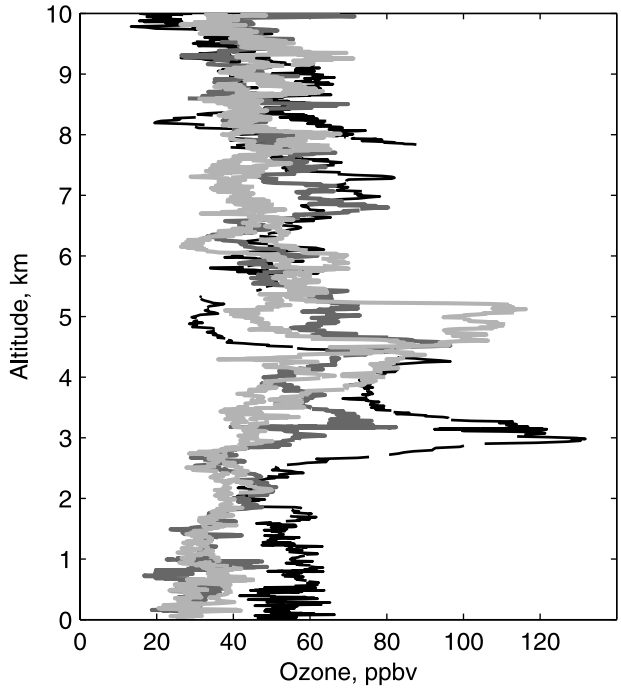

Figure 7. G-IV 1-s ozone measurements during descent from 0100 to 0200 UTC, 10 March (black line), descent from 0300 to 0400 UTC, 12 March (dark gray line), and ascent and descent between 1900 UTC, 12 March, and 0400 UTC, 13 March (light gray line).

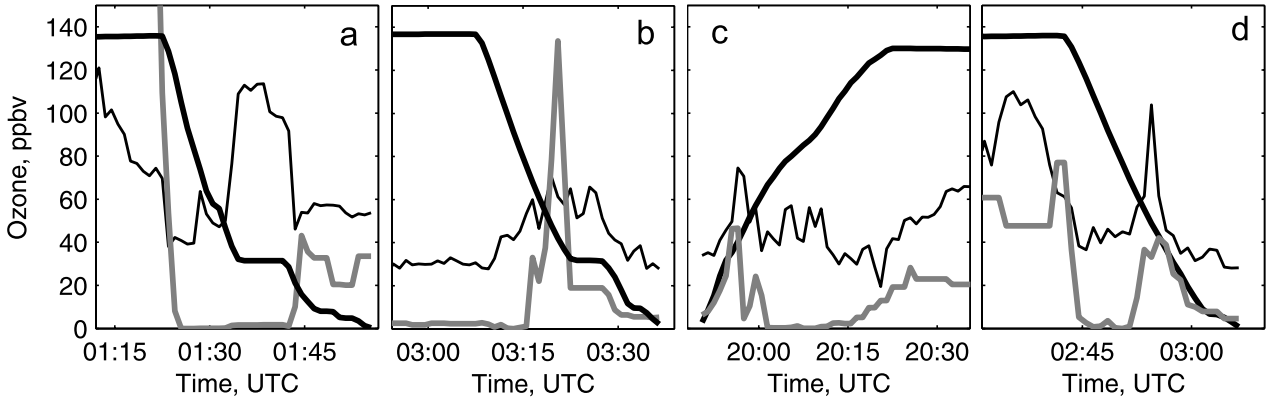

Figure 8. Minute-averaged ozone (thin black line), G-IV altitude (m/100, thick black line), and FLEXPART stratospheric ozone tracer (gray line) for (a) aircraft descent on 10 March, (b) aircraft descent on 12 March, (c) aircraft ascent on 12 March, and (d) aircraft descent on 13 March.

reaching a maximum of 115 ppbv at 0400 UTC, 10 March (CO data were missing). Figure 6a compares the ozone measurements to the FLEXPART tracer. The tracer has a much smaller peak of 42 ppbv, occurring one hour after the ozone maximum at MLO. The maximum FLEXPART tracer (95 ppbv) lags the maximum MLO ozone value (115 ppbv) by 15 hours and is too low by 20 ppbv, not including the fraction of tropospheric ozone that would have been mixed into the air mass. Figure 9 shows a three-dimensional view of the FLEXPART tracer's 40 ppbv isosurface at the time of the MLO ozone maximum. An animated version of Figure 9 (not shown), spanning the 7–13 March period, shows the intrusion swept over MLO from the north and indicates that the FLEXPART tracer captured the major ozone fluctuations at MLO within a degree of latitude or longitude and/or within a lag time of about 15 hours.

[30] The 10 March event also had a stronger impact on Honolulu. Ozone reached 60 ppbv at 0000 UTC, 10 March, the highest ozone value measured at Honolulu during the first six months of 2004. This 60 ppbv value occurred at 1400 LT when photochemical ozone production would be relatively efficient, but ozone was already above 50 the night before and during the morning, so any photochemical production would have occurred on top of an elevated background ozone. Figure 6b shows that the timing of the measured ozone fluctuations at Honolulu corresponds to the FLEXPART stratospheric tracer fluctuations from 9 March through 11 March. The stratospheric tracer mixing ratios are lower than the measured values, which are the likely result of mixing between background tropospheric ozone and the remnants of the stratospheric intrusion. The ozone increase at Honolulu on 9 March occurs approximately 24 hours earlier than the ozone peak at MLO, in agreement with the earlier discussion of the 10 March event having its maximum influence near the surface one day earlier than its maximum influence throughout the tropospheric column.

3.3. Comparison to Ozone Climatology

[31] The measurements from the G-IV, MLO and Honolulu were compared to the long-term records to gauge the relative strength of these stratospheric intrusions. Figure 10 compares the 1-s G-IV measurements on 29 February to the

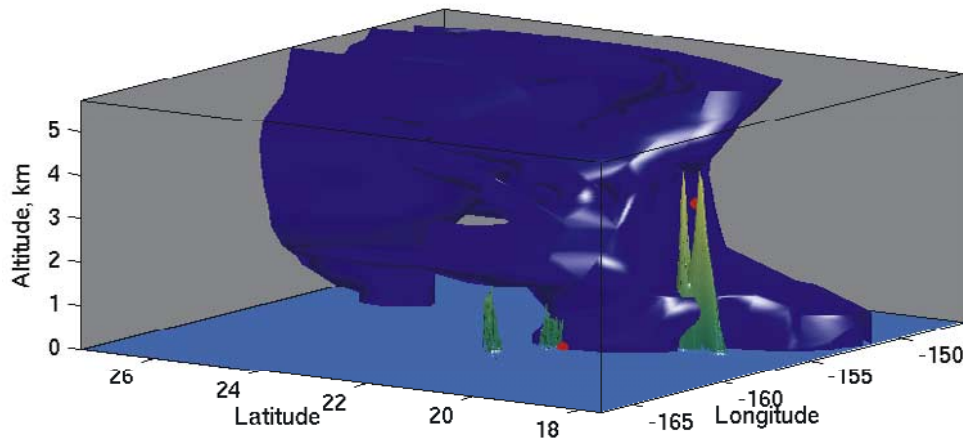

Figure 9. Three-dimensional view of the 40 ppbv isosurface of the FLEXPART stratospheric ozone tracer at 0400 UTC, 10 March 2004. The terrain of Hawaii is shown in green, and the locations of Honolulu (sea level) and MLO (3400 m) are indicated by the red circles.

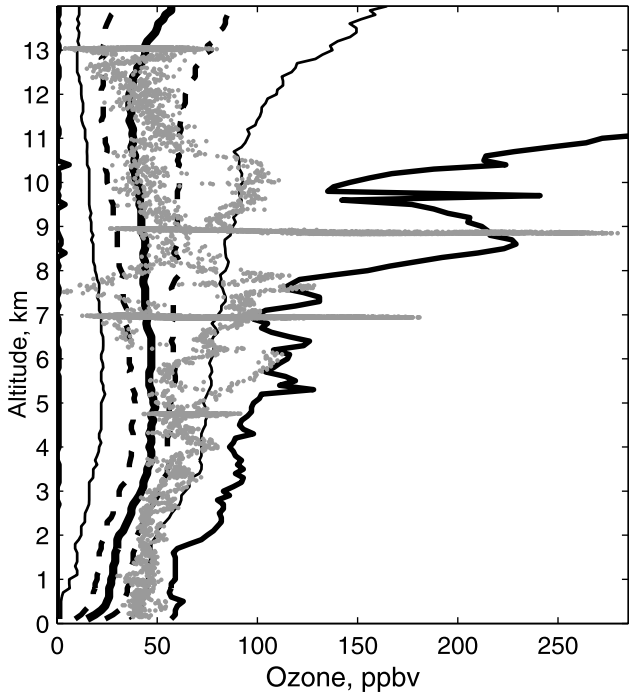

Figure 10. Comparison between the 1-s G-IV ozone data (gray circles) on 29 February 2004 and the 100-m vertical resolution 1991–2004 ozonesonde climatology at Hilo, Hawaii. Hilo data are summarized as median values (thick line), 25th and 75th percentiles (dashed lines), 5th and 95th percentiles (thin lines), and minimum and maximum values (medium-weight lines).

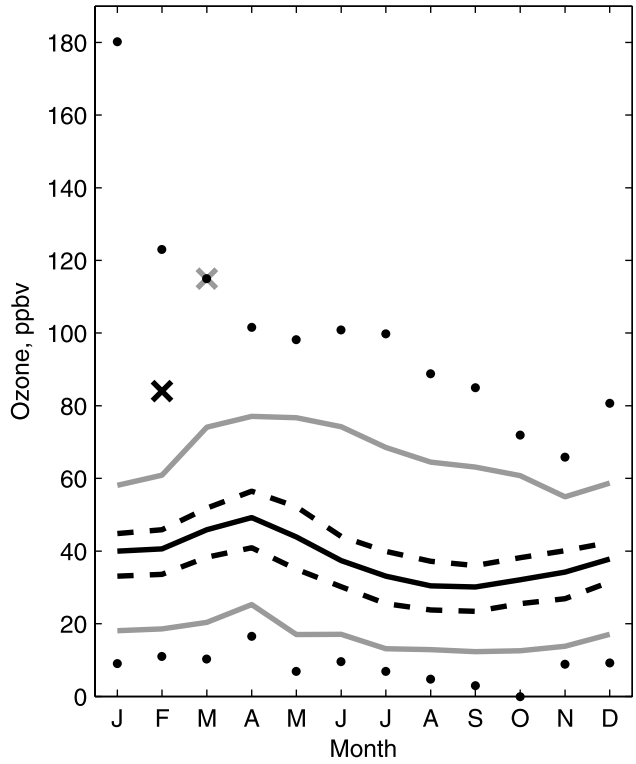

Figure 11. MLO hourly average ozone climatology from 1973 to 2004 represented as monthly median values (black line), 25th and 75th percentiles (dashed lines), 1st and 99th percentiles (gray lines), and minimum and maximum values (circles). The maximum hourly values on 29 February 2004 (black cross) and 10 March 2004 (gray cross) are also shown.

1991–2004 ozonesonde record at Hilo, Hawaii (100 m vertical resolution). The G-IV measurements at 8.9 km and 6.9 km are greater than the corresponding ozonesonde maximum values by 60 and 80 ppbv, respectively. We also compared the 29 February G-IV measurements to the 1982–1991 Hilo ozonesonde record (not shown), which is limited by a coarser vertical resolution, and found similar results. The peak of 72 ppbv at 3.3 km, as well as many values below 2 km, is greater than the Hilo 95th percentile. Similar results were found for the 10 March flight with the ozone peak of 132 ppbv at 3 km exceeding the maximum Hilo value by more than 40 ppbv (compare Figures 7 and 10).

[32] Figure 11, created from the full 1973–2004 MLO ozone record, shows the monthly ozone distribution at MLO illustrating the springtime maximum typical of tropical locations. The ozone peak of 81 ppbv on 29 February is much greater than the February 99th percentile, and the ozone peak of 115 ppbv on 10 March equals the previous maximum value for March. While Honolulu resides in the marine boundary layer its 1994–2003 ozone climatology also exhibits a springtime maximum (Figure 12). The ozone peak of 45 ppbv on 29 February is just below the 99th percentile, and the ozone peak of 60 ppbv on 10 March is greater than the previous 1994–2003 March maximum.

[33] To determine if 2004 was an anomalous year for stratospheric intrusions, we compared 22 G-IV ozone profiles from January–March 2004 to the January–March ozonesonde record at Hilo for the years 1991–2004 (150 profiles). We excluded all G-IV profiles that specifically targeted stratospheric intrusions. All G-IV and ozonesonde profiles were converted to 1 km layer averages. Then for each kilometer layer between 0 and 13 km we compared the

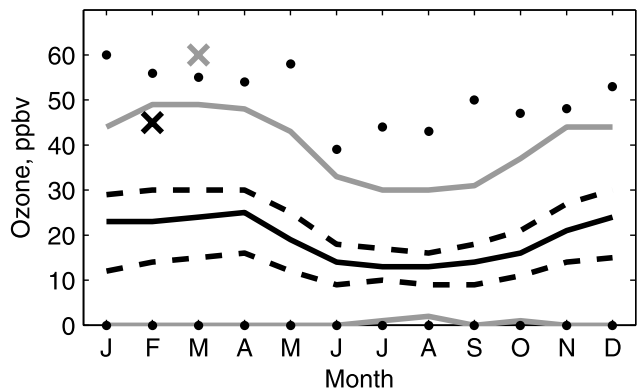

Figure 12. Honolulu hourly average ozone climatology from 1994 to 2003 represented as monthly median values (black line), 25th and 75th percentiles (dashed lines), 1st and 99th percentiles (gray lines), and minimum and maximum values (circles). The maximum hourly values on 29 February 2004 (black cross) and 10 March 2004 (gray cross) are also shown.

ozone distributions of the two data sets using the Kruskal-Wallace nonparametric one-way analysis of variance test.

[34] The only layers with significantly different ozone distributions at the 95% confidence interval were the 0–1, 11–12 and 12–13 km layers. Below 1 km, ozone measured by the G-IV was significantly greater than ozone measured by the sondes. At this altitude range the G-IV was in the vicinity of Honolulu, which has much greater anthropogenic emissions than Hilo, Hawaii. The greater ozone in 2004 could be due to local ozone production near Honolulu, or it could be due to a greater downward flux of free tropospheric and/or stratospheric ozone. We extracted water vapor mixing ratio profiles every 6 hours from the NCEP GFS model above Hilo and compared January–March 2004 to a 5-year climatology of January–March values from 2000 to 2004. The lower troposphere had greater values of water vapor mixing ratios in 2004, suggesting that transport from the upper/troposphere and lower stratosphere did not have a greater influence in 2004. Between 11 and 13 km the G-IV profiles showed significantly more ozone in 2004. Given the greater incidence of ozone values above 100 ppbv we could assume that the difference is likely due to a greater stratospheric influence at these altitudes in 2004. However, we compared the 2004 PV profiles (also extracted from the NCEP GFS model) above Hilo to the 2000–2004 climatology and found no statistically significant difference in the PV distribution in the middle and upper troposphere. The greater ozone measured by the G-IV could be due to the large amount of horizontal distance that it covers, making it more likely to intercept intrusions than an ozonesonde (see below for further discussion).

[35] In summary, ozone during 2004 was not significantly different from the 1991–2004 ozone record, between 1 and 11 km. While the G-IV measured significantly more ozone below 1 km and between 11 and 13 km in comparison to the long-term Hilo ozonesonde record, analysis of the water vapor mixing ratio and PV profiles above Hilo does not indicate that the greater ozone values are due to an anomalously greater occurrence of stratospheric intrusions in 2004.

4. Discussion

[36] *Baray et al.* [2003] suggested that the decay of large stratospheric intrusions in the tropics would be important to the tropical troposphere ozone budget. The results from our study support their hypothesis to some extent. FLEXPART calculated that the 29 February and 10 March intrusions transported 1.14 and 1.75 Tg of ozone into the tropical troposphere, respectively (Table 1). Because the intrusions became detached from the polar jet stream, were located beneath the tropical tropopause, and decayed in the tropics we assume that all of the ozone in these intrusions was irreversibly mixed into the troposphere. However, their impact on the tropics is not so clear. High concentrations of ozone tracer from the 29 February event reached as far south as 10°N and remnants eventually advected toward the equator. The animation of the 29 February event shows that some of the lower portions of this intrusion were advected northward out of the tropics after the occurrence of the maximum amount of ozone transported into the tropics. Over time most of the decayed intrusion was finally advected out of the tropics toward the northeast into the extratropics ahead of the next approaching longwave trough, so this particular midlatitude intrusion only had a temporary effect on the tropics.

[37] In contrast, most of the ozone tracer from the 10 March event remained in the northerly portions of the tropics, although some high-concentration fragments reached as far south as 5°N, while others were advected into the extratropics by midlatitude troughs. The 1.75 Tg within the 10 March intrusion is a very large amount of ozone to be dumped into the troposphere in a single event, especially in comparison to the global net stratosphere-to-troposphere ozone flux, which has been estimated to range from 391 to 846 Tg per year [*Hauglustaine et al.*, 1998]. In comparison, *Cooper et al.* [2004] analyzed a large stratospheric intrusion over the North Pacific Ocean during May 2002. They estimated that below 12 km the intrusion contained 5.2 Tg of ozone. Over the next 7.5 days the intrusion decayed as it flowed along the polar jet stream, which is typical for a midlatitude intrusion. However, most of the ozone remained in the stratosphere on the northern side of the polar jet stream. Only 0.5 Tg was irreversibly transported into the troposphere over the 7.5 day time period.

[38] Regardless of whether or not midlatitude intrusions like the 29 February or 10 March events remain in the tropics, their evolution has important ramifications for the tropospheric ozone budget in general. The fact that intrusions penetrating into the tropics become detached from the polar jet stream and subsequently become surrounded on all sides by tropical air with a 16 km tropopause, implies that the typical intrusion reaching the tropics will inject more ozone into the troposphere than the typical intrusion that remains near the polar jet stream in the midlatitudes. An exception would be a large midlatitude cutoff low that remains detached from the polar front and decays in the midlatitudes [*Bamber et al.*, 1984; *Price and Vaughan*, 1993; *Gouget et al.*, 2000].

[39] In terms of stratospheric intrusion decay, one mechanism that has been explored in midlatitudes is convective erosion [*Langford and Reid*, 1998], which can actually be triggered by the potential vorticity anomaly within the intrusion [*Danielsen*, 1964; *Griffiths et al.*, 2000]. This process is especially important for the erosion of the lowered tropopause within cutoff lows [*Price and Vaughan*, 1993]. While studies have shown that intrusions into the tropics trigger deep convection along the leading edge of the PV anomaly [*Kiladis*, 1998; *Waugh and Funatsu*, 2003], our analysis has shown that the relatively cold midlatitude air advected into the tropics destabilized the atmosphere beneath the PV anomaly allowing convective clouds to erode the base of the intrusion and mix stratospheric ozone into the troposphere.

[40] The analyses in section 3.3 showed that transport effects on ozone were not anomalous during January–March 2004, and that we can expect to find strong midlatitude intrusions that penetrate into the tropical middle and lower troposphere in other winters. However, if this is true, why are these two events outliers with respect to the Hilo ozonesonde record? Random chance could be part of the answer as the 10 March intrusion is by itself an anomalous event as shown by comparison to the MLO and Honolulu

ozone records. However, differences in sampling techniques could also play a role. First, consider the limited sampling of the ozonesondes. For example, between 1991 and 2004 there were 648 ozonesonde launches from Hilo. The typical ozonesonde rises at the rate of 5 m/s, which means the sonde spends 200 s in any given 1000 m layer. So the 1000 m layer at 8–9 km above Hawaii has been sampled by ozonesondes for a total of 36 hours during the last 13 years, or 0.03% of the time. When this exercise is limited to just the January–March time period, the ozonesondes have only sampled the 8–9 km layer for approximately 9 hours. While the G-IV did not spend quite as much time in the 8–9 km layer, it did specifically target intrusions at this altitude and its airspeed of 220 m/s allowed it to cover a large horizontal distance, which ozonesondes cannot accomplish. Second, these intrusions are often associated with severe weather and ozonesondes are not usually launched in high-wind or high-rainfall conditions to avoid damage to the balloon and instrument payload. Given the limited sampling duration of the ozonesondes, their limited horizontal range and their avoidance of severe weather conditions, perhaps it is not surprising that the Hilo ozonesondes have not yet measured ozone as great as 280 ppbv at 8–9 km as was seen on the 29 February flight that specifically targeted the most intense region of a stratospheric intrusion.

5. Conclusions

[41] The new findings from this study are as follows: (1) Lagrangian dispersion models can forecast, with a high degree of accuracy, the locations of midlatitude stratospheric intrusions as they penetrate into the middle and lower troposphere of the tropics. (2) Targeted aircraft sampling of such an intrusion revealed the strongest free tropospheric ozone enhancements ever measured above Hawaii in comparison to a 22-year ozonesonde record. (3) Cold air advection associated with the transport of the intrusion into the tropics produced convective clouds that eroded the base of the 29 February intrusion, which mixed stratospheric ozone into the tropical troposphere. (4) Agreement between the FLEXPART stratospheric ozone tracer and measured ozone fluctuations at Mauna Loa and Honolulu show that these intrusions can influence ozone mixing ratios in the lower troposphere and marine boundary layer of the tropics. (5) Transport conditions during winter 2004 were not anomalous, and although the 10 March intrusion was an extreme event, the direct transport of midlatitude stratospheric ozone into the lower troposphere and marine boundary layer of the tropical Pacific Ocean can be expected in any winter. (6) We suggest that stratospheric intrusions that break away from the polar jet stream as they advect into the tropics are more effective at transporting ozone into the troposphere than intrusions that remain close to the polar jet stream in midlatitudes.

[42] In terms of future studies, a full understanding of the magnitude, structure and lifetime of stratospheric intrusions within the tropics and their impact on the tropical and extratropical ozone budget requires targeted aircraft measurements. Ideally an aircraft would be dedicated to sampling an intrusion on sequential days as it decays in the tropics and descends into the marine boundary layer. An onboard ozone lidar and measurements of other trace gases such as CO, NO_y and even HCl, which has been shown to be a good tracer of stratospheric air [*Marcy et al.*, 2004], would help discern the stratospheric contribution to the tropospheric ozone budget. Given the limited flight time of the G-IV jet aircraft in the lower troposphere, a low-altitude propeller aircraft and/or a lidar instrumented aircraft would be better suited for tracking intrusions just above and within the marine boundary layer.

[43] **Acknowledgments.** We thank Donna Sueper at the NOAA Aeronomy Laboratory for preparing the final aircraft and dropsonde data and Kenneth Aikin, also at the NOAA Aeronomy Laboratory, for reducing the final ozone data. Bill Kuster of the NOAA Aeronomy Laboratory maintained the ozone instrument during the experiment. We also thank P. Novelli at NOAA CMDL for providing the Mauna Loa Observatory CO data, and the Air Surveillance and Analysis Section of the Hawaii State Department of Health for providing the 2004 Honolulu ozone data. Ozone and CO data measured by in-service Airbus aircraft were provided by the MOZAIC program. The U.S. Environmental Protection Agency is acknowledged for making the 1994–2003 Honolulu ozone record available on its Air Quality System database. GOES satellite imagery, NEXRAD imagery, and NCEP GFS gridded meteorological fields were provided by UNIDATA Internet delivery and displayed using UNIDATA McIDAS software. Finally, we thank the Data Support Section of NCAR's Scientific Computing Division for making the final run of the 2000–2004 NCEP GFS analyses available for download.

References

Bamber, D. J., P. G. W. Healey, B. M. R. Jones, S. A. Penkett, A. F. Tuck, and G. Vaughan (1984), Vertical profiles of tropospheric gases: Chemical consequences of stratospheric intrusions, *Atmos. Environ.*, *18*, 1759–1766.

Baray, J.-L., V. Daniel, G. Ancellet, and B. Legras (2000), Planetary-scale tropopause folds in the southern subtropics, *Geophys. Res. Lett.*, *27*, 353–356.

Baray, J. L., S. Baldy, R. D. Diab, and J. P. Cammas (2003), Dynamical study of a tropical cut-off low over South Africa, and its impact on tropospheric ozone, *Atmos. Environ.*, *37*, 1475–1488.

Betts, A. K., L. V. Gatti, A. M. Cordova, M. A. F. Silva Dias, and J. D. Fuentes (2002), Transport of ozone to the surface by convective downdrafts at night, *J. Geophys. Res.*, *107*(D20), 8046, doi:10.1029/2000JD000158.

Browell, E. V., et al. (1996), Large-scale air mass characteristics observed over western Pacific Ocean during summertime, *J. Geophys. Res.*, *101*, 1691–1712.

Browell, E. V., et al. (2001), Large-scale air mass characteristics observed over the remote tropical Pacific Ocean during March–April 1999: Results from PEM-Tropics B field experiment, *J. Geophys. Res.*, *106*, 32,481–32,501.

Cooper, O. R., et al. (2004), On the life-cycle of a stratospheric intrusion and its dispersion into polluted warm conveyor belts, *J. Geophys. Res.*, *109*, D23S09, doi:10.1029/2003JD004006.

Danielsen, E. F. (1964), Report on Project Springfield, *DASA 1517*, 97 pp., Def. At. Support Agency, Washington, D. C.

Eckhardt, S., A. Stohl, S. Beirle, N. Spichtinger, P. James, C. Forster, C. Junker, T. Wagner, U. Platt, and S. Jennings (2003), The North Atlantic Oscillation controls air pollution transport to the Arctic, *Atmos. Chem. Phys.*, *3*, 1769–1778.

Emanuel, K. A. (1994), *Atmospheric Convection*, Oxford Univ. Press, New York.

Emanuel, K. A., and M. Živković-Rothman (1999), Development and evaluation of a convection scheme for use in climate models, *J. Atmos. Sci.*, *56*, 1766–1782.

Fishman, J., C. E. Watson, J. C. Larsen, and J. A. Logan (1990), Distribution of tropospheric ozone determined from satellite data, *J. Geophys. Res.*, *95*, 3599–3617.

Forster, C., et al. (2001), Transport of boreal forest fire emissions from Canada to Europe, *J. Geophys. Res.*, *106*, 22,887–22,906.

Forster, C., et al. (2004), Lagrangian transport model forecasts and a transport climatology for the Intercontinental Transport and Chemical Transformation 2002 (ITCT 2K2) measurement campaign, *J. Geophys. Res.*, *109*, D07S92, doi:10.1029/2003JD003589.

Fujiwara, M., et al. (2003), Ozonesonde observations in the Indonesian maritime continent: A case study on ozone rich layer in the equatorial upper troposphere, *Atmos. Environ.*, *37*, 353–362.

Gouget, H., G. Vaughan, A. Marenco, and H. G. J. Smit (2000), Decay of a cut-off low and contribution to stratosphere-troposphere exchange, *Q. J. R. Meteorol. Soc.*, *126*, 1117–1141.

Griffiths, M., A. J. Thorpe, and K. A. Browning (2000), Convective destabilization by a tropopause fold diagnosed using potential-vorticity inversion, *Q. J. R. Meteorol. Soc.*, *126*, 125–144.

Hahn, C. J., J. Y. Merrill, and B. G. Mendonca (1992), Meteorological influences during MLOPEX, *J. Geophys. Res.*, *97*, 10,291–10,309.

Hauglustaine, D. A., G. P. Brasseur, S. Walters, P. J. Rasche, J.-F. Müller, L. K. Emmons, and M. A. Carroll (1998), MOZART, a global chemical transport model for ozone and related chemical tracers: 2. Model results and evaluation, *J. Geophys. Res.*, *103*, 28,291–28,335.

Hübler, G., et al. (1992), Total reactive oxidized nitrogen (NO_y) in the remote Pacific troposphere and its correlation with O_3 and CO: Mauna Loa Observatory Photochemistry Experiment 1988, *J. Geophys. Res.*, *97*, 10,427–10,447.

James, P., A. Stohl, C. Forster, S. Eckhardt, P. Seibert, and A. Frank (2003), A 15-year climatology of stratosphere-troposphere exchange with a Lagrangian particle dispersion model: 2. Mean climate and seasonal variability, *J. Geophys. Res.*, *108*(D12), 8522, doi:10.1029/2002JD002639.

Kiladis, G. N. (1998), Observations of Rossby waves linked to convection over the eastern tropical Pacific, *J. Atmos. Sci.*, *55*, 321–339.

Komhyr, W. D. (1969), Electrochemical cells for gas analysis, *Ann. Geophys.*, *25*, 203–210.

Komhyr, W. D., R. A. Barnes, G. B. Brothers, J. A. Lathrop, and D. P. Opperman (1995), Electrochemical concentration cell ozonesonde performance evaluation during STOIC 1989, *J. Geophys. Res.*, *100*, 9231–9244.

Ladstätter-Weißenmayer, A., J. Meyer-Arnek, A. Schlemm, and J. P. Burrows (2004), Influence of stratospheric airmasses on tropospheric vertical O_3 columns based on GOME (Global Ozone Monitoring Experiment) measurements and backtrajectory calculation over the Pacific, *Atmos. Chem. Phys.*, *4*, 903–909.

Langford, A. O., and S. J. Reid (1998), Dissipation and mixing of a small-scale stratospheric intrusion in the upper troposphere, *J. Geophys. Res.*, *103*, 31,265–31,276.

Lelieveld, J., et al. (2001), The Indian Ocean Experiment: Widespread air pollution from south and Southeast Asia, *Science*, *291*, 1031–1036.

Lelieveld, J., J. van Aardenne, H. Fischer, M. de Reus, J. Williams, and P. Winkler (2004), Increasing ozone over the Atlantic Ocean, *Science*, *302*, 1483–1487.

Liu, H., D. J. Jacob, L. Y. Chan, S. J. Oltmans, I. Bey, R. M. Yantosca, J. M. Harris, B. N. Duncan, and R. V. Martin (2002), Sources of tropospheric ozone along the Asian Pacific Rim: An analysis of ozonesonde observations, *J. Geophys. Res.*, *107*(D21), 4573, doi:10.1029/2001JD002005.

Marcy, T. P., et al. (2004), Quantifying stratospheric ozone in the upper troposphere with in situ measurements of HCl, *Science*, *304*, 261–265.

Moody, J. L., A. J. Wimmers, and J. C. Davenport (1999), Remotely sensed specific humidity: Development of a derived product from the GOES Imager Channel 3, *Geophys. Res. Lett.*, *26*, 59–62.

National Oceanic and Atmospheric Administration (2004), Climatological data: Hawaii and Pacific, February 2004, vol. 100, no. 02, http://www5.ncdc.noaa.gov/pubs/publications.html#CD, Natl. Clim. Data Cent., Asheville, N. C.

Nedelec, P., J.-P. Cammas, V. Thouret, G. Athier, J.-M. Cousin, C. Legrand, C. Abonnel, F. Lecoeur, G. Cayez, and C. Marizy (2003), An improved infrared carbon monoxide analyser for routine measurements aboard commercial Airbus aircraft: Technical validation and first scientific results of the MOZAIC III programme, *Atmos. Chem. Phys.*, *3*, 1551–1564.

Oltmans, S. J., et al. (1996), Summer and spring ozone profiles over the North Atlantic from ozonesonde measurements, *J. Geophys. Res.*, *101*, 29,179–29,200.

Oltmans, S. J., et al. (2004), Tropospheric ozone over the North Pacific from ozonesonde observations, *J. Geophys. Res.*, *109*, D15S01, doi:10.1029/2003JD003466.

Otkin, J. A., and J. E. Martin (2004), A synoptic climatology of the subtropical kona storm, *Mon. Weather Rev.*, *132*, 1502–1517.

Postel, G. A., and M. H. Hitchman (1999), A climatology of Rossby wave breaking along the subtropical tropopause, *J. Atmos. Sci.*, *56*, 359–373.

Price, J. D., and G. Vaughan (1993), The potential for stratosphere-troposphere exchange in cut-off low systems, *Q. J. R. Meteorol. Soc.*, *119*, 343–365.

Proffitt, M. H., and R. C. McLaughlin (1983), Fast-response dual-beam UV-absorption ozone photometer suitable for use in stratospheric balloons, *Rev. Sci. Instrum.*, *54*, 1719–1728.

Scott, R. K., J.-P. Cammas, and C. Stolle (2001), Stratospheric filamentation into the upper tropical troposphere, *J. Geophys. Res.*, *106*, 11,835–11,848.

Seibert, P., B. Krüger, and A. Frank (2001), Parametrisation of convective mixing in a Lagrangian particle dispersion model, paper presented at 5th GLOREAM Workshop, Paul Scherrer Inst., Wengen, Switzerland, 24–26 Sept.

Stohl, A., and D. J. Thomson (1999), A density correction for Lagrangian particle dispersion models, *Boundary Layer Meteorol.*, *90*, 155–167.

Stohl, A., and T. Trickl (1999), A textbook example of long-range transport: Simultaneous observation of ozone maxima of stratospheric and North American origin in the free troposphere over Europe, *J. Geophys. Res.*, *104*, 30,445–30,462.

Stohl, A., M. Hittenberger, and G. Wotawa (1998), Validation of the Lagrangian particle dispersion model FLEXPART against large scale tracer experiment data, *Atmos. Environ.*, *24*, 4245–4264.

Stohl, A., N. Spichtinger-Rakowsky, P. Bonasoni, H. Feldmann, M. Memmesheimer, H. E. Scheel, T. Trickl, S. H. Hübener, W. Ringer, and M. Mandl (2000), The influence of stratospheric intrusions on alpine ozone concentrations, *Atmos. Environ.*, *34*, 1323–1354.

Stohl, A., S. Eckhardt, C. Forster, P. James, and N. Spichtinger (2002), On the pathways and timescales of intercontinental air pollution transport, *J. Geophys. Res.*, *107*(D23), 4684, doi:10.1029/2001JD001396.

Stohl, A., C. Forster, S. Eckhardt, N. Spichtinger, H. Huntrieser, J. Heland, H. Schlager, S. Wilhelm, F. Arnold, and O. Cooper (2003), A backward modeling study of intercontinental pollution transport using aircraft measurements, *J. Geophys. Res.*, *108*(D12), 4370, doi:10.1029/2002JD002862.

Stoller, P., et al. (1999), Measurements of atmospheric layers from the NASA DC-8 and P-3B aircraft during PEM-Tropics A, *J. Geophys. Res.*, *104*, 5745–5764.

Thompson, A. M., J. C. Witte, R. D. Hudson, H. Guo, J. R. Herman, and M. Fujiwara (2001), Tropical tropospheric ozone and biomass burning, *Science*, *291*, 2128–2132.

Thompson, A. M., et al. (2003), Southern Hemisphere Additional Ozonesondes (SHADOZ) 1998–2000 tropical climatology: 2. Tropospheric variability and the zonal wave-one, *J. Geophys. Res.*, *108*(D2), 8241, doi:10.1029/2002JD002241.

Thouret, V., J. Y. N. Cho, R. E. Newell, A. Marenco, and H. G. J. Smit (2000), General characteristics of tropospheric trace constituent layers observed in the MOZAIC program, *J. Geophys. Res.*, *105*, 17,379–17,392.

Thouret, V., J. Y. N. Cho, M. J. Evans, R. E. Newell, M. A. Avery, J. D. W. Barrick, G. W. Sachse, and G. L. Gregory (2001), Tropospheric ozone layers observed during PEM-Tropics B, *J. Geophys. Res.*, *106*, 32,527–32,538.

Tuck, A. F., et al. (1997), The Brewer-Dobson circulation in the light of high altitude in situ aircraft observations, *Q. J. R. Meteorol. Soc.*, *123*, 1–69.

Waugh, D. W., and B. M. Funatsu (2003), Intrusions into the tropical upper troposphere: Three-dimensional structure and accompanying ozone and OLR distributions, *J. Atmos. Sci.*, *60*, 637–653.

Waugh, D. W., and L. M. Polvani (2000), Climatology of intrusions into the tropical upper troposphere, *Geophys. Res. Lett.*, *27*, 3857–3860.

Weller, R., R. Lilischkis, O. Schrems, R. Neuber, and S. Wessel (1996), Vertical ozone distribution in the marine atmosphere over the central Atlantic Ocean (56°S–50°N), *J. Geophys. Res.*, *101*, 1387–1399.

Wesely, M. L. (1989), Parameterization of surface resistances to gaseous dry deposition in regional-scale models, *Atmos. Environ.*, *23*, 1293–1304.

Wimmers, A. J., and J. L. Moody (2004), Tropopause folding at satellite-observed spatial gradients: 2. Development of an empirical model, *J. Geophys. Res.*, *109*, D19307, doi:10.1029/2003JD004146.

O. R. Cooper, E. Y. Hsie, G. Hübler, G. N. Kiladis, D. D. Parrish, and A. F. Tuck, NOAA Aeronomy Laboratory, 325 Broadway, Boulder, CO 80305, USA. (owen.r.cooper@noaa.gov)

B. J. Johnson and S. J. Oltmans, NOAA Climate Monitoring and Diagnostics Laboratory, 325 Broadway, R/GMD1, Boulder, CO 80305-3328, USA.

A. S. Lefohn, A.S.L. & Associates, 111 North Last Chance Gulch, Suite 4A, Helena, MT 59601, USA.

J. L. Moody, Department of Environmental Sciences, University of Virginia, Clark Hall, 291 McCormick Road, P. O. Box 400123, Charlottesville, VA 22904-4123, USA.

M. Shapiro, NOAA-UCAR, 3450 Mitchell Lane, Boulder, CO 80301, USA.

A. Stohl, Department of Regional and Global Pollution Issues, NILU, P. O. Box 100, N-2027 Kjeller, Norway.